


Cite this: *CrystEngComm*, 2022, 24, 1292

Too much water? Not enough? *In situ* monitoring of the mechanochemical reaction of copper salts with dicyandiamide†

Lucia Casali,^a Torvid Feiler,^b Maria Heilmann,^b Dario Braga,^a Franziska Emmerling^{iD}*^b and Fabrizia Grepioni^{iD}*^a

In situ monitoring of mechanochemical reactions between dicyandiamide (DCD) and CuX_2 salts ($\text{X} = \text{Cl}^-$, NO_3^-), for the preparation of compounds of agrochemical interest, showed the appearance of a number of phases. It is demonstrated that milling conditions, such as the amount of water added in wet grinding and/or the milling frequency, may affect the course of the mechanochemical reactions, and drive the reaction towards the formation of different products. It has been possible to discover by *in situ* monitored experiments two novel crystalline forms, namely the neutral complexes $[\text{Cu}(\text{DCD})_2(\text{OH})_2(\text{NO}_3)_2]$ (**2**) and $[\text{Cu}(\text{DCD})_2(\text{OH})_2\text{Cl}_2] \cdot \text{H}_2\text{O}$ (**4**), in addition to the previously known molecular salt $[\text{Cu}(\text{DCD})_2(\text{OH})_2][\text{NO}_3]_2 \cdot 2\text{H}_2\text{O}$ (**1**, DIVWAG) and neutral complex $[\text{Cu}(\text{DCD})_2(\text{OH})_2\text{Cl}_2]$ (**3**, AQCUCU), for which no synthesis conditions were available. Compounds **2** and **4** were fully characterized via a combination of solid-state techniques, including X-ray diffraction, Raman spectroscopy and TGA.

Received 15th December 2021,
Accepted 17th January 2022

DOI: 10.1039/d1ce01670a

rsc.li/crystengcomm

Introduction

In recent years the search for eco-sustainable methods has become increasingly urgent,¹ given the economic and environmental impact of traditional industrial processes, which are generally based on a massive use of environmentally problematic and hazardous solvents.

Among the eco-sustainable methods mechanochemistry stands out,^{2,3} as it is a synthetic approach promoted by the input of mechanical energy in the absence (grinding) or in the presence (kneading) of a minimum amount of solvent, thus overcoming solvent-related problems such as solubility and solvolysis typically found in solution chemistry. The mechanochemical method can provide a wide spectrum of materials,⁴ ranging from metal-organic complexes to novel organic molecules, regardless of the relative solubilities of the starting components. In addition to this, the success of mechanochemistry is due to fast and quantitative reactions, along with a simple implementation.

In light of this, mechanochemistry has attracted significant interest as an alternative method for obtaining

pure compounds.⁵ Despite the wide application, the mechanisms of milling reactions are still not fully understood. Typically, mechanistic information is deduced from *ex situ* experiments in a stepwise manner: milling is interrupted at fixed time intervals, the milling vessel opened, and the sample removed for *ex situ* analysis. However, this procedure unavoidably affects the reaction conditions, and air-sensitive or fast converting intermediates/phase changes cannot be detected under these conditions. Therefore, the ability to monitor these reactions directly *in situ*, without the need to interrupt the milling process, helps in the detection, isolation, and characterization of new phases/intermediates, as also in the optimization of the synthetic procedure.⁶

In this work we investigate the mechanochemical synthesis of metal-organic complexes through the combination of *in situ* techniques, *i.e.* time-resolved X-ray diffraction (XRD) coupled with Raman spectroscopy,^{7,8} which provide real-time information about the solid-state transformations occurring during the milling process. The investigated complexes, based on copper(II) and dicyandiamide (DCD), are intended for agrochemical applications in the context of a more sustainable agriculture. Copper(II) serves the dual purpose of micronutrient and inhibitor towards urease,⁹ the soil enzyme responsible of the fast hydrolysis of urea into ammonium. DCD, on the other side, is supplied to the soil with the aim of inhibiting ammonia monooxygenase (AMO),¹⁰ which catalyzes the conversion of ammonium into hydroxylamine (NH_2OH), precursor of greenhouse gases such as NO_2 , NO .¹¹ We have

^a Department of Chemistry "G. Ciamician", University of Bologna, 40126 Bologna, Italy. E-mail: fabrizia.grepioni@unibo.it

^b BAM Federal Institute for Materials Research and Testing, 12489 Berlin, Germany. E-mail: franziska.emmerling@bam.de

† Electronic supplementary information (ESI) available: X-ray powder patterns, Rietveld refinements, Raman spectra, TGA, DSC. CCDC 2128518 and 2128519. For ESI and crystallographic data in CIF or other electronic format see DOI: 10.1039/d1ce01670a



already shown that mechanochemically synthesized co-crystals of urea could represent a novel class of fertilizers, proving that co-crystallization can be a new promising route for the delivery of agrochemicals.^{12–14} Moreover, it was recently shown that *in situ* monitoring of mechanochemical reactions is a powerful approach to explore the solid-state reactivity of agrochemicals.¹⁵

To this goal we selected from the CSD database two coordination complexes based on DCD and copper salts, *i.e.* [Cu(DCD)₂(OH₂)₂][NO₃]₂·2H₂O (**1**) (refcode DIVWAG¹⁶) and [Cu(DCD)₂(OH₂)₂Cl₂] (**3**) (refcode AQCYCU¹⁷). For both compounds, however, no details could be found on synthetic procedures and conditions; as single crystal data are deposited in the CSD structural database, it is likely that the two compounds were obtained from solution. We decided to try a mechanochemical approach, as *in situ* Raman spectroscopy in monitoring the mechanochemical synthesis of DCD-based coordination compounds had proven to be efficacious in the case of zinc complexes.¹⁸ Our results show that the milling conditions affect the course of the mechanochemical reactions, with different phases appearing depending on the amount of the milling water and on the grinding conditions. In addition to the known compounds **1** and **3**, novel crystalline forms, *i.e.* the neutral complexes [Cu(DCD)₂(OH₂)₂(NO₃)₂] (**2**) and [Cu(DCD)₂(OH₂)Cl₂]·H₂O (**4**) were detected, isolated and structurally characterized *via* solid-state methods. Analogous syntheses were conducted for sake of comparison in aqueous solution or *via* slurry in water (see below).

The *in situ* strategy for the simultaneous, real-time analysis of milling reactions is thus a powerful tool for the (i) isolation and characterization of new materials, (ii) optimization of the synthetic procedure, and (iii) understanding of the reactivity of the investigated systems, thus highlighting the advantages of mechanochemistry over conventional synthetic methods.

Experimental section

Materials

All reagents were purchased from Sigma-Aldrich and used without further purification.

Solid-state synthesis (MCE group at Unibo)

DCD and Cu(NO₃)₂·3H₂O. Pure crystalline **1** was synthesized by reacting DCD (32.83 mg, 0.40 mmol) and Cu(NO₃)₂·3H₂O (47.17 mg, 0.20 mmol) in a 2:1 stoichiometric ratio in a mixer mill MM 200, at 20 Hz for 60 minutes; an agate jar was utilized, with two 5 mm agate balls, and 100 μL of water were added to the initial solid mixture. The same procedure, without the addition of water, was adopted for the preparation of pure compound **2**.

DCD and CuCl₂·2H₂O. DCD (39.73 mg, 0.40 mmol) and CuCl₂·2H₂O (47.17 mg, 0.20 mmol) in a 2:1 stoichiometric ratio were reacted in a mixer mill MM 200 at 20 Hz for 10 minutes with 100 μL of water, resulting in the formation of

compound **3**. Pure crystalline **4** was obtained by manual grinding of the reagents with mortar and pestle for 2 minutes.

Solid-state synthesis (Helmholtz Centre Berlin for Materials and Energy)

DCD and Cu(NO₃)₂·3H₂O. The mechanochemical reaction between DCD (32.83 mg, 0.40 mmol) and Cu(NO₃)₂·3H₂O (47.17 mg, 0.20 mmol), performed in a vibration ball mill (Pulverisette 23, Fritsch, Germany) at 50 Hz in a Perspex jar with two 4 mm steel balls, yielded pure compound **1** *via* the addition of 80 μL of milling water. By reducing the milling water to 20 μL, pure crystalline **2** was obtained.

DCD and CuCl₂·2H₂O. The mechanochemical reaction between DCD (39.73 mg, 0.40 mmol) and CuCl₂·2H₂O (47.17 mg, 0.20 mmol) performed at 50 Hz in a Perspex jar with one 7 mm zirconia ball afforded pure compound **3** *via* the addition of 80 μL of milling water. In the absence of milling water an unidentified compound **X** was obtained (see Results and discussion).

Solution synthesis

DCD and Cu(NO₃)₂·3H₂O. Solvent evaporation from a water solution of DCD (32.83 mg, 0.40 mmol) and Cu(NO₃)₂·3H₂O (47.17 mg, 0.20 mmol) yielded a physical mixture of **1** and **2**.

DCD and CuCl₂·2H₂O. A physical mixture of **3** and **X** was obtained by following the same procedure (39.73 mg of DCD and 40.27 mg of CuCl₂·2H₂O).

Slurry method

DCD and Cu(NO₃)₂·3H₂O. Water (*ca.* 1 mL) was added dropwise to a physical mixture of DCD (0.41 g) and Cu(NO₃)₂·3H₂O (0.58 g) in a 2:1 stoichiometry. When a suspension was obtained that could easily be stirred, the addition of water was interrupted, and the suspension was stirred for 3 days at ambient conditions. Finally, the suspension was filtered and dried, and identified as compound **2** *via* X-ray diffraction.

DCD and CuCl₂·2H₂O. The same procedure was employed to prepare **4** starting from a 2:1 physical mixture of DCD and CuCl₂·2H₂O (0.49 g and 0.51 g, respectively).

X-ray diffraction from powder

For phase identification purposes. X-ray powder diffraction (XRPD) patterns on **1**, **2**, **3** and **4** were collected on a PANalytical X'Pert Pro Automated diffractometer equipped with an X'celerator detector in Bragg–Brentano geometry, using the Cu-Kα radiation ($\lambda = 1.5418 \text{ \AA}$) without monochromator in the 5–50° 2θ range (step size 0.033°; time per step: 20 s; soller slit 0.04 rad, antiscatter slit: 1/2, divergence slit: 1/4 ; 40 mA × 40 kV).



Structural characterization from powder data

Room temperature X-ray powder diffraction (XRPD) patterns for **2** and **4** were collected in transmission geometry on a PANalytical X'Pert PRO automated diffractometer equipped with Focusing mirror and Pixcel detector in the 2θ range $3-70^\circ$ (step size 0.0130° , time/step 118.32 s, Vx 40 kV \times 40 mA). Data analyses were carried out using the PANalytical X'Pert Highscore Plus program. The identity of the bulk materials obtained *via* solid-state processes was always verified by comparison of calculated and observed powder diffraction patterns. Powder diffraction data for **2** and **4** were analyzed with the software PANalytical X'Pert HighScore Plus. Unit cell parameters were found using DICVOL4 algorithm. Both structures were solved *via* simulated annealing, performed with EXPO2014 (**2** in the space group $P\bar{1}$ and **4** in the space group $P2_1/c$). Ten runs for simulated annealing trials were set, and a cooling rate (defined as the ratio T_n/T_{n-1}) of 0.95 was used. In both cases the best solution was chosen for Rietveld refinement, which was performed with the software TOPAS5.0.¹⁹ A shifted Chebyshev function with 8 parameters and a pseudo-Voigt function were used to fit background and peak shape, respectively. All the hydrogen atoms were fixed in calculated positions with the software Mercury. Rietveld refinements for the two structures are collected in the ESI†

Thermogravimetric analysis (TGA)

TGA measurements for all samples (*ca.* 10 mg of DCD, **1**, **2**, **3** and **4**) were performed using a PerkinElmer TGA7 thermogravimetric analyzer, in the $30-300^\circ\text{C}$ temperature range, under a N_2 gas flow at a heating rate of $5.00^\circ\text{C min}^{-1}$.

Differential scanning calorimetry (DSC)

DSC traces were recorded with a PerkinElmer Diamond differential scanning calorimeter. All samples (*ca.* 10 mg of DCD, **1**, **2**, **3** and **4**) were placed in open Al-pans. All measurements were conducted in the $50-240^\circ\text{C}$ temperature range, at a heating rate of $5.00^\circ\text{C min}^{-1}$.

In situ Raman spectroscopy

Raman measurements were performed on a Raman RXN1™ analyser (Kaiser Optical Systems, France). A non-contact probe head with a working distance of 6 cm (spot size = 1 mm) and an excitation wavelength of $\lambda = 785$ nm was used for the collection of Raman spectra every 30 s. For every measurement five spectra, with an acquisition time of 5 s, were accumulated.

In situ synchrotron X-ray diffraction

In situ X-ray diffraction measurements were performed at 5 s intervals at the μSpot beamline (BESSY II, Helmholtz Centre Berlin for Materials and Energy). The reactions were carried out in a vibration ball mill (Pulverisette 23, Fritsch, Germany) using a custom-made Perspex grinding jar. The experiments

were conducted with a wavelength of 0.7314 \AA using a double crystal monochromator (Si 111).⁷ The obtained scattering images were integrated with the Dpdak-software.²⁰ The resulting X-ray diffraction patterns (2θ vs. intensity) with $\lambda = 0.7314 \text{ \AA}$ were corrected for background.

Results and discussion

DCD and $\text{Cu}(\text{NO}_3)_2 \cdot 3\text{H}_2\text{O}$

Preliminary reactions conducted at UniBO between DCD and $\text{Cu}(\text{NO}_3)_2$ with small, but variable quantities of water resulted in the known compound $[\text{Cu}(\text{DCD})_2(\text{OH}_2)_2][\text{NO}_3]_2 \cdot 2\text{H}_2\text{O}$ (**1**) (DIVWAG), but extra peaks were always present (see ESI†), which could not be attributed to the reagents and were later identified as the new form $[\text{Cu}(\text{DCD})_2(\text{OH}_2)_2(\text{NO}_3)_2]$ (**2**). The synthesis was repeated several times, but the outcome was never reproducible. In order to better understand the reaction mechanism, we followed the structural evolution over time at the μSpot beamline BESSY II (Helmholtz Centre Berlin for Materials and Energy), *via* the *in situ* tandem combination of X-ray diffraction with Raman spectroscopy. The mechanochemical reaction was performed at 50 Hz with $50 \mu\text{L}$ of milling water in a Perspex jar, chosen as the material does not interfere with data collection. As shown in Fig. 1, the formation of the known compound **1** was almost instantaneous, with the peaks of the reagents not even detectable. Interestingly, the new crystalline form **2** started to appear within the first minutes, and after *ca.* 6 minutes it was the only crystalline form present (Fig. 1, left). *In situ* Raman spectroscopy showed some changes in the absorption profile at the same time interval of the phase transition (Fig. 1, right, and ESI†). The band of **1** at 2270 cm^{-1} starts to decrease in intensity concomitantly with the appearance of a

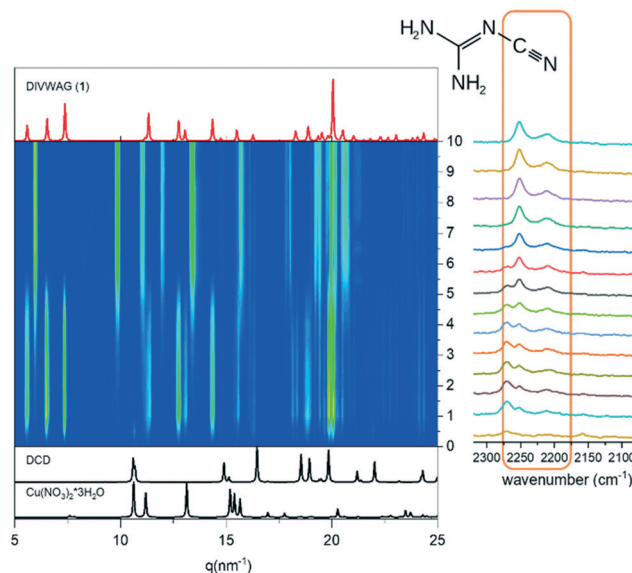


Fig. 1 Time-evolution of the milling reaction between DCD and $\text{Cu}(\text{NO}_3)_2 \cdot 3\text{H}_2\text{O}$: powder X-ray diffraction (left) coupled with Raman spectroscopy (right).



new band at 2250 cm^{-1} . The band under consideration corresponds to the frequency of the asymmetric stretching of the $\text{N}-\text{C}\equiv\text{N}$ group of DCD.²¹

In **1** the N_{imino} atoms belonging to DCD molecules are directly coordinated to the copper ion, which is in a square planar geometry (see Fig. 2). Therefore, the variation in the absorption of this vibrational mode is reasonably due to a variation in the coordination network involving DCD, with a concomitant change of the coordination geometry around copper, possibly related to a variation in the content of the crystallization water. The mechanochemical reaction was then performed with different amounts of milling water (Fig. 3), and we found out that the formation of **1**, as also the kinetics of formation, is correlated to the amount of milling water. In the absence of water pure solid **2** was invariably obtained as soon as the reaction started. By addition of water, up to $10\text{ }\mu\text{L}$, compound **1** was first obtained, but after two minutes it converted into **2**. Finally, with the addition of $80\text{ }\mu\text{L}$ of water, compound **1** formed immediately, and remained stable for the whole duration of the experiment. This trend is in agreement with a transformation of **1** into **2** following the release of crystallization water.

The milling frequency also affected the kinetics of the reaction: by reducing the milling frequency to 20 Hz , while keeping constant the water amount at $50\text{ }\mu\text{L}$, the lifetime of compound **1** increased to *ca.* 60 minutes, against the 5 minutes observed for the mechanochemical reaction at 50 Hz (see ESI†).

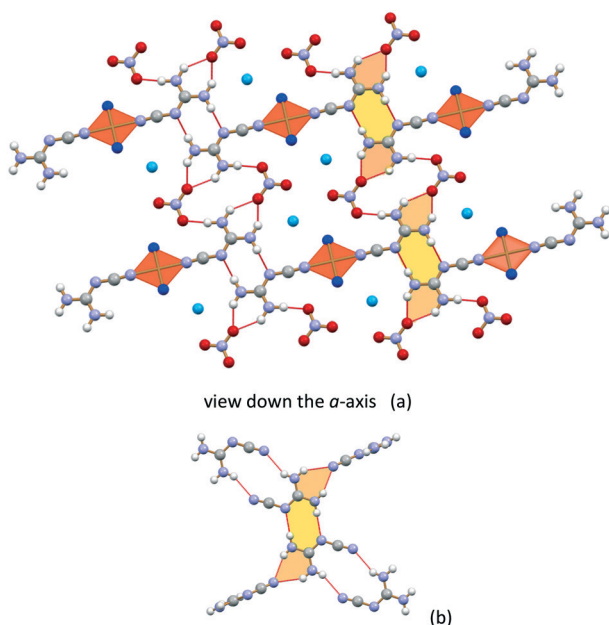


Fig. 2 (a) Relevant packing features in crystalline **1** (DIVWAG): the copper ion is in a square planar geometry, with two water molecules and the N_{imino} atoms belonging to DCD molecules at the vertices of the square. The DCD molecules form the same type of hydrogen bonded dimers (in yellow) observed in pure DCD (CYAMPD11). (b). Hydrogen bonded ring motives evidenced in pale orange in (b) are also present in **1**, but involve the nitrate ions (a).

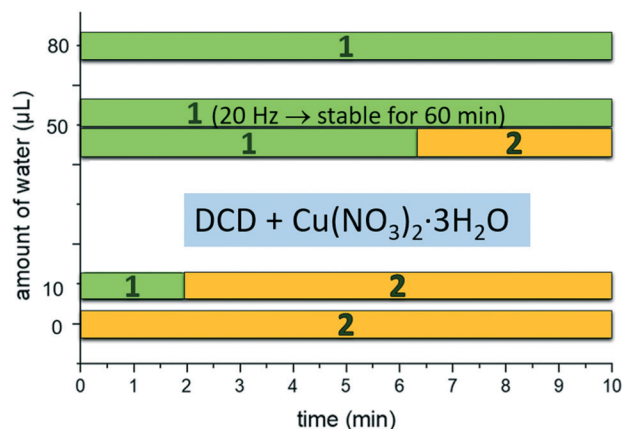
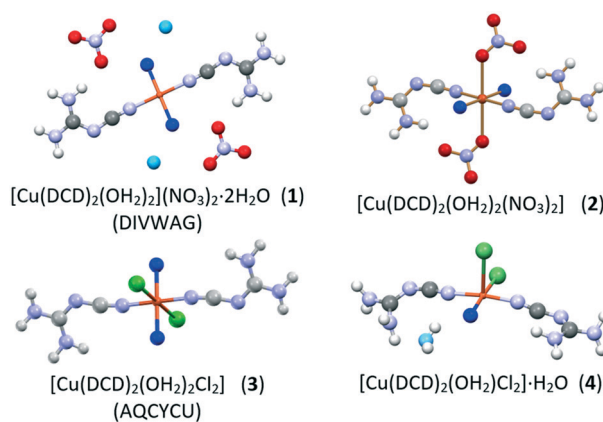


Fig. 3 *In situ* monitoring of formation and stability of compounds **1** and **2** as a function of time and amount of milling water. Milling frequency 50 Hz (unless differently specified).

TGA measurements on **1** and **2** evidence the difference in the water content and in the interaction of the water molecules with the copper cation (see ESI†). The TGA trace for **1** shows two weight losses, one in the range $60\text{--}80\text{ }^{\circ}\text{C}$ and the second in the range $100\text{--}120\text{ }^{\circ}\text{C}$, corresponding to a stepwise dehydration process, involving first the two water molecules on the second coordination sphere, then the two water molecules directly linked to the copper cation. The TGA trace of **2**, on the contrary, only presents an event at $100\text{--}120\text{ }^{\circ}\text{C}$, corresponding to the loss of two water molecules, thus indicating that compound **2** is a dihydrate and the water molecules are likely bound to the metal center; this information was crucial for the structural determination of **2** from powder diffraction data (see Scheme 1 and Fig. 4).

The DCD molecules are organized in hydrogen bonded dimers with the nitrate anions, which act as hydrogen bond acceptors of the double $\text{N}-\text{H}_{\text{DCD}}$ donor [$\text{N}(\text{H})_{\text{DCD}}\cdots\text{O}^-$ $2.924(3)\text{ }\text{\AA}$ and $3.068(3)\text{ }\text{\AA}$]. Such crystal arrangement is consistent with the data in the CSD database: among the 7 structures containing DCD and nitrate ions, only DIVWAG (**1**) does not



Scheme 1 Schematic representation of the compounds discussed in this work (O_{W} atoms bound/not bound to the metal cations are in blue/cyan, respectively).



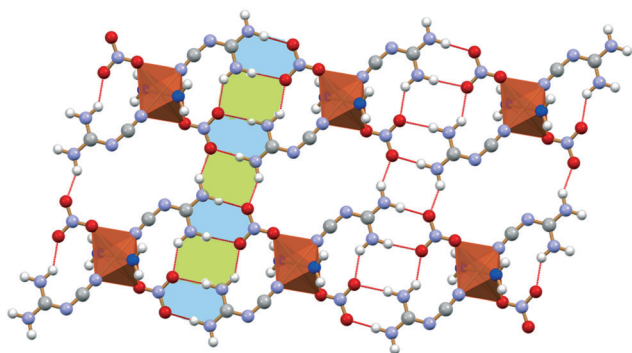


Fig. 4 Hydrogen bonding patterns in crystalline $[\text{Cu}(\text{DCD})_2(\text{OH}_2)_2(\text{NO}_3)_2]$: no direct interactions are observed between DCD molecules (compare with Fig. 1), as the hydrogen bonding DCD dimers present in crystalline 1 are replaced here by dimers between DCD molecules and nitrate anions. Additional HB-rings involving the NO_3^- ions are evidenced in light green.

display this kind of interaction. Such crystal arrangement results in the formation of parallel layers of the dimers (one layer is shown in Fig. 4), connected to each other *via* the water molecules $[\text{C}-\text{N}_{\text{DCD}} \cdots (\text{H})\text{O}_{\text{water}} \ 2.839(2) \ \text{\AA}$ and $\text{N}-\text{O}^-_{\text{nitrate}} \cdots (\text{H})\text{O}_{\text{water}} \ 2.815(2) \ \text{\AA}]$.

A solution synthesis and a slurry in water were also performed with hydrated copper nitrate and DCD. Crystallization from an aqueous solution of the two reagents yielded a physical mixture of compounds 1 and 2; no single crystals of 2 were obtained. The slurry experiment, on the other hand, yielded pure compound 2, as this is the thermodynamically stable phase in the presence of water (see ESI†).

DCD and $\text{CuCl}_2 \cdot 2\text{H}_2\text{O}$

DCD and $\text{CuCl}_2 \cdot 2\text{H}_2\text{O}$ were mixed in a 2:1 stoichiometric ratio in an agate jar, and reacted in a mixer mill MM 200 at 20 Hz in the presence of variable amounts of water. The synthesis resulted in the known compound 3 (AQCYCU), regardless of the milling time (10 to 90 minutes). However, given the important information that may arise from *in situ* monitoring, we decided to follow the structural evolution over time of the mechanochemical reaction between DCD and $\text{CuCl}_2 \cdot 2\text{H}_2\text{O}$ at 50 Hz with 50 μL of water at the μSpot beamline BESSY II (Fig. 5).

The formation of the expected compound 3 was almost instantaneous, to the point that the peaks of the reagents were not detectable; the formation of 3, however, was accompanied by the concomitant formation of an unknown crystalline form, named X, which disappeared within the first 60 seconds.

In order to identify form X, we performed the same mechanochemical synthesis with a lesser amount of milling water: in this way the lifetime of X increased, to the point that, in the absence of water, it became the only crystalline form present. Interestingly, pure solid X transforms into a

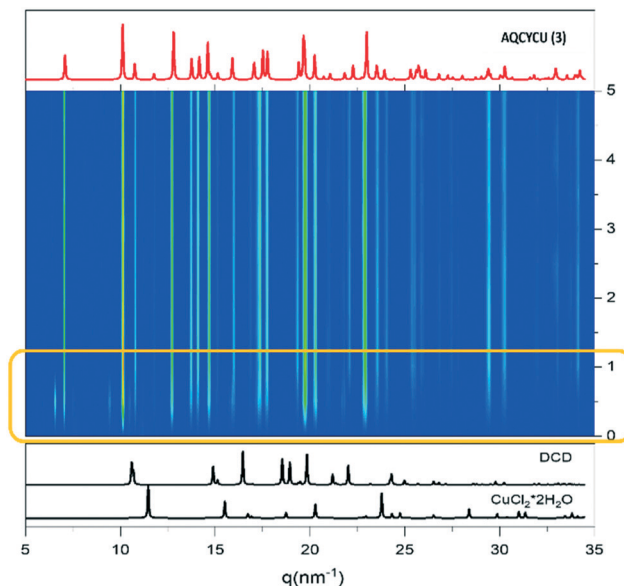


Fig. 5 Time evolution of the milling reaction between DCD and $\text{CuCl}_2 \cdot 2\text{H}_2\text{O}$ with 50 μL of water at 50 Hz. The appearance of the phase X is highlighted by the orange rectangle.

physical mixture of X and of the new compound $[\text{Cu}(\text{DCD})_2(\text{OH}_2)\text{Cl}_2] \cdot \text{H}_2\text{O}$ (4) upon exposure to air.

Manual grinding at ambient conditions – with no intentional addition of water – yielded pure solid 4 (Fig. 6): manual grinding in open air evidently caused stoichiometric water uptake from the atmosphere.

Finally, for sake of comparison, we performed the synthesis from a water solution of the reagents and *via* slurry. The first method yielded a physical mixture of 3 and X, in agreement with the mechanochemical synthesis in the presence of water. Interestingly, the slurry method resulted solely in the formation of compound 4 (see ESI†).

TGA analysis performed on powder of pure form 4 proved that the compound contains two water molecules (see ESI†), as in the case of 3. The difference between the two compounds could be evidenced upon structural resolution from powder X-ray data. (see ESI†): Compounds 3 and 4,

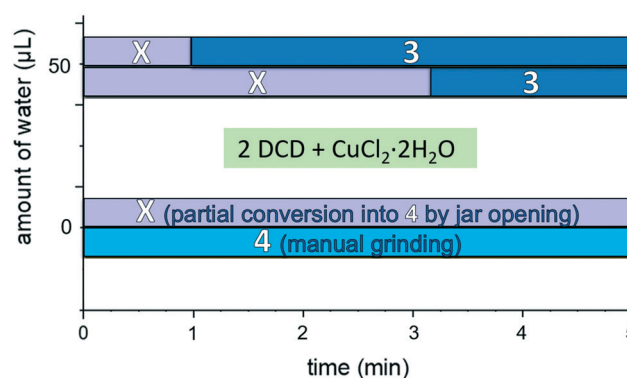


Fig. 6 *In situ* monitoring of formation and stability of compounds X, 3 and 4 as a function of time and amount of milling water. Milling frequency 50 Hz.



although sharing the same stoichiometry, differ for the coordination geometry around the copper cation, which changes from octahedral in **3** to square-pyramidal in **4** (Scheme 1), as one of the two coordinated water molecules in **3** becomes a crystallization water molecule in **4** (see Fig. 7 for a comparison of the two packing arrangements).

The copper cation in crystalline **4** is bound to two DCD ligands, one water molecule and two chloride anions. A second water molecule interacts exclusively with the first water molecule and one DCD molecule. The crystallographically independent DCD molecules are involved in different hydrogen bond networks: one of the molecules is hydrogen bond acceptor of the non-coordinated water [$C-N_{DCD} \cdots (H)O_{water}$ 2.783(4) Å], while the second molecule is hydrogen bond donor toward the non-coordinated water molecule [$N(H)_{DCD} \cdots O_{water}$ 2.928(4) Å] and two chloride anions in equatorial position [$N(H)_{DCD} \cdots Cl^-$ 3.211(1) Å and 3.256(5) Å]. The chloride anion in the axial position is instead the hydrogen bond acceptor of the coordinated water molecule [$O(H)_{water} \cdots Cl^-$ 3.211(4) Å]. All these interactions

result in the formation of hydrogen bonded wavy chains, which are held together by hydrogen bonds between the axial chloride anions and the coordinated water molecule, giving rise to a wavy layered packing (Fig. 7a). This packing arrangement can be compared with the one of crystalline **3** (Fig. 7b), where DCD molecules interact directly with each other along infinite HB-chains, which interact on one side with the copper cations, and on the other side with the chloride anions, thus forming layers, as shown in the bottom part of Fig. 7b.

Conclusions

In this work we investigated the solid-state reactivity of DCD and CuX_2 salts ($X = Cl^-, NO_3^-$), compounds employed in the agrochemical field to tackle the nitrification issue, by *in situ* monitoring of the mechanochemical reactions.

With regard to DCD and $Cu(NO_3)_2 \cdot 3H_2O$, the first attempted mechanochemical reactions always provided different outcomes, *i.e.* the pure compound **1** or a physical mixture of **1** and **2** in different proportions. The combination of X-ray diffraction with Raman spectroscopy allowed us to (i) isolate and characterize the new compound **2**, (ii) understand the relationship between the two phases and (iii) optimize the synthetic procedure to obtain pure **1** or **2**, along with the understanding that the amount of milling water deeply influenced the kinetics as also the outcome of the synthesis.

Concerning DCD and $CuCl_2 \cdot 2H_2O$, all the mechanochemical syntheses provided the expected compound **3**. However, *in situ* monitoring *via* X-ray diffraction revealed the appearance of a transient phase **X**, whose lifetime depended on the amount of milling water. In attempting to isolate this phase, a new phase **4** was obtained by manual grinding of the reagents and characterized through solid-state methods.

The presented case-studies underlined the importance of a precise synthetic protocol describing the mechanochemical synthesis. The explored systems turned out to be highly sensitive to the amount of water or the milling conditions. When performing mechanochemical reactions, a generic reference to a catalytic amount of milling water may thus be imprecise; the use of unspecified water addition, together with the use of only one milling frequency, may prevent the discovery of products only accessible through the utilization of different reaction conditions.

Along with the benefits arising from *in situ* strategies, in this work we also highlighted the advantages of the mechanochemical method over solution ones. For both complexes the synthesis from solution always (i) resulted in a physical mixture of different phases and (ii) never provided single crystals of the new compounds, while our mechanochemical approach allowed the preparation and characterization of pure crystalline compounds. Work is in progress to expand this strategy to additional hydrate metal systems.

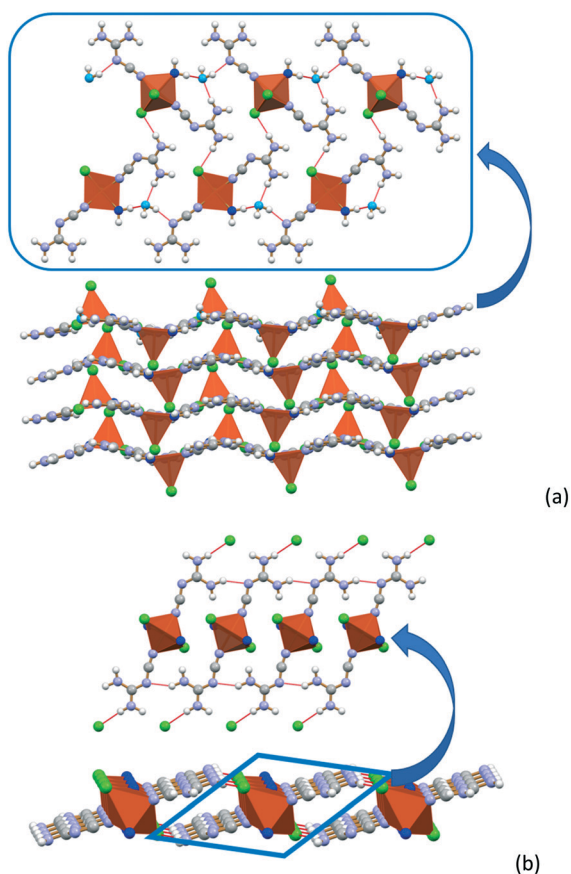


Fig. 7 Hydrogen bonding patterns (a) in the layered structure of crystalline **4**: the DCD molecules do not interact with each other, but form H-bonds with water molecules and chloride ions. (b) Compare with arrangement in crystalline **3** (only a portion of the packing is shown here), where chains of hydrogen bonded DCD molecules interact on one side with the copper cations and on the other side with the chloride anions.



Author contributions

L. C. performed the syntheses and the solid-state characterization. T. F. and M. H. collected the *in situ* measurements and performed the data treatment. F. G. and F. E. conceived, designed and supervised the whole project. All authors contributed to the preparation of the manuscript.

Conflicts of interest

There are no conflicts to declare.

Acknowledgements

We acknowledge financial support from the Chemistry Department “G. Ciamician” (L.C., Marco Polo grant). We thank Max Rautenberg for his help in data treatment.

Notes and references

- 1 C. J. Clarke, W. C. Tu, O. Levers, A. Bröhl and J. P. Hallett, *Chem. Rev.*, 2018, **118**, 747–800.
- 2 T. Friščić, C. Mottillo and H. M. Titi, *Angew. Chem.*, 2020, **132**, 1030–1041.
- 3 K. J. Ardila-Fierro and J. G. Hernández, *ChemSusChem*, 2021, **14**, 2145–2162.
- 4 S. Quaresma, P. C. Alves, P. Rijo, M. T. Duarte and V. André, *Molecules*, 2021, **26**, 1904–1922.
- 5 S. L. James, C. J. Adams, C. Bolm, D. Braga, P. Collier, T. Friščić, F. Grepioni, K. D. M. Harris, G. Hyett, W. Jones, A. Krebs, J. Mack, L. Maini, A. G. Orpen, I. P. Parkin, W. C. Shearouse, J. W. Steed and D. C. Waddell, *Chem. Soc. Rev.*, 2012, **41**, 413–447.
- 6 P. A. Julien, K. Užarević, A. D. Katsenis, S. A. J. Kimber, T. Wang, O. K. Farha, Y. Zhang, J. Casaban, L. S. Germann, M. Etter, R. E. Dinnebier, S. L. James, I. Halasz and T. Friščić, *J. Am. Chem. Soc.*, 2016, **138**, 2929–2932.
- 7 L. Batzdorf, F. Fischer, M. Wilke, K.-J. Wenzel and F. Emmerling, *Angew. Chem.*, 2015, **127**, 1819–1822.
- 8 H. Kulla, S. Haferkamp, I. Akhmetova, M. Röllig, C. Maierhofer, K. Rademann and F. Emmerling, *Angew. Chem., Int. Ed.*, 2018, **57**, 5930–5933.
- 9 X. Dong, Y. Li, Z. Li, Y. Cui and H. Zhu, *J. Inorg. Biochem.*, 2012, **108**, 22–29.
- 10 F. Musiani, V. Broll, E. Evangelisti and S. Ciurli, *J. Biol. Inorg. Chem.*, 2020, **25**, 995–1007.
- 11 F. Beeckman, H. Motte and T. Beeckman, *Curr. Opin. Biotechnol.*, 2018, **50**, 166–173.
- 12 L. Casali, L. Mazzei, O. Shemchuk, K. Honer, F. Grepioni, S. Ciurli, D. Braga and J. Baltrusaitis, *Chem. Commun.*, 2018, **54**, 7637–7640.
- 13 L. Casali, L. Mazzei, O. Shemchuk, L. Sharma, K. Honer, F. Grepioni, S. Ciurli, D. Braga and J. Baltrusaitis, *ACS Sustainable Chem. Eng.*, 2019, **7**, 2852–2859.
- 14 L. Mazzei, V. Broll, L. Casali, M. Silva, D. Braga, F. Grepioni, J. Baltrusaitis and S. Ciurli, *ACS Sustainable Chem. Eng.*, 2019, **7**, 13369–13378.
- 15 P. A. Julien, L. S. Germann, H. M. Titi, M. Etter, R. E. Dinnebier, L. Sharma, J. Baltrusaitis and T. Friščić, *Chem. Sci.*, 2020, **11**, 2350–2355.
- 16 M. J. Begley, P. Hubberstey and C. H. M. Moore, *J. Chem. Res.*, 1985, (S) **378**, (M) 4001.
- 17 A. Chiesi, L. Coghi, A. Mangia, M. Nardelli and G. Pelizzi, *Acta Crystallogr., Sect. B: Struct. Crystallogr. Cryst. Chem.*, 1971, **27**, 192–197.
- 18 V. Trukil, L. Fábíán, D. G. Reid, M. J. Duer, G. J. Jackson, M. Eckert-Maksić and T. Friščić, *Chem. Commun.*, 2010, **46**, 9191–9193.
- 19 A. A. Coelho, *J. Appl. Crystallogr.*, 2018, **51**, 210–218.
- 20 G. Benecke, W. Wagermaier, C. Li, M. Schwartzkopf, G. Flucke, R. Hoerth, I. Zizak, M. Burghammer, E. Metwalli, P. Müller-Buschbaum, M. Trebbin, S. Förster, O. Paris, S. V. Roth and P. Fratzl, *J. Appl. Crystallogr.*, 2014, **47**, 1797–1803.
- 21 X. Lin, W. L. J. Hasi, X. T. Lou, S. Q. G. W. Han, D. Y. Lin and Z. W. Lu, *Anal. Methods*, 2015, **7**, 3869–3875.

